located in the range of $\Lambda = (240, 260)$, regardless of the streamwise location, and correspond to a vortex bigger than the most amplified vortex in the case of the first mode. It should be noted that the critical vortex corresponds to $\Lambda_{cr} = 251.1$. The cutoff wavelength parameter, defining the lower bound of the unstable wavelengths, is $\Lambda_c = 75.14$ and is higher than the cutoff wavelength for the first mode ($\Lambda_c = 44.29$).[1] This suggests that conditions exist under which the only admissible form of the unstable motion is the one consisting of a single layer of vortices. The comparison of the total growth of the first mode vs the second mode is given in Fig. 3. The results suggest that the total amplification of the second mode is insignificant in comparison to the first mode. Figure 4 illustrates the variations of the total amplification as a function of Görtler number for vortices corresponding to $\Lambda = 120$, 650, and 1250.[1] It may be concluded that while the total amplification of the second mode is considerably smaller than the total amplification of the first mode, the growth process is qualitatively unaffected.

Conclusions

The growth process of the second mode of the Görtler instability of the Blasius boundary layer has been studied. The results suggest that the second mode is more stable than the first mode, over the entire wavelength range. The growth process of the second mode is considerably slower than that of the first; therefore, the second mode is not likely to be observed experimentally.

Acknowledgments

This work was supported by a grant from the Natural Sciences and Engineering Research Council of Canada. The author would like to thank Mr. G. C. Ng for performing the computations.

References

[1]Floryan, J. M. and Saric, W. S., "Wavelength Selection and Growth of Görtler Vortices," *AIAA Journal*, Vol. 22, Nov. 1984, pp. 1529-1538.

[2]Floryan, J. M. and Saric, W. S., "Stability of Görtler Vortices in Boundary Layers," *AIAA Journal*, Vol. 20, March 1983, pp. 316-324.

Dynamic Condensation for Structural Redesign

Ki-Ook Kim*
Automated Analysis Corporation
Ann Arbor, Michigan

Introduction

THE modification of the modal characteristics such as frequencies and mode shapes is of interest in many areas of structural redesign. For frequency control, an energy method with a Rayleigh quotient is usually used. Stetson et al.[1,2] used a first-order perturbation equation for energy balance.

For large changes, nonlinear terms must be included.[3] The equilibrium equation is used to modify mode shapes. While the equilibrium equation approach gives exact results, it has many unknowns in large systems, which is unacceptable for mathematical programming techniques.

The modal condensation method, which transforms the original space into a subspace spanned by the lowest modes, is simple for frequency changes. However, the method requires several redesign analyses because the subspace generates lower frequencies than the desired goals.[4]

The present study explores the application of dynamic condensation[5,6] to the modification of modal characterisics of undamped mechanical systems. The accuracy of dynamic condensation methods usually does not depend on the choice of master degrees of freedom, which is an advantage over static condensation. The method puts emphasis on mode shape changes as well as frequency changes.

Dynamic Condensation

The equation of motion of an undamped system is

$$[k]\{\phi\} = [m]\{\phi\}\lambda \tag{1}$$

where $[k]$ and $[m]$ are the stiffness and mass matrices and λ and $\{\phi\}$ the eigenvalue and eigenvector of the system, respectively. Equation (1) can be expressed in compact form as

$$[D]\{\phi\} = \{0\} \tag{2}$$

where $[D] = [k] - \lambda[m]$ is the dynamic stiffness matrix. Equation (2) is partitioned as

$$\begin{bmatrix} D_{ss} & D_{sm} \\ D_{ms} & D_{mm} \end{bmatrix} \begin{Bmatrix} \phi_s \\ \phi_m \end{Bmatrix} = \begin{Bmatrix} 0 \\ 0 \end{Bmatrix} \tag{3}$$

where $\{\phi_s\}$ and $\{\phi_m\}$ are the slave and master sets of degrees of freedom, respectively.

The equation of the perturbed system is

$$\begin{bmatrix} D'_{ss} & D'_{sm} \\ D'_{ms} & D'_{mm} \end{bmatrix} \begin{Bmatrix} \phi'_s \\ \phi'_m \end{Bmatrix} = \begin{Bmatrix} 0 \\ 0 \end{Bmatrix} \tag{4}$$

or

$$[D_{ss}']\{\phi_s'\} + [D_{sm}']\{\phi_m'\} = \{0\} \tag{5a}$$

$$[D_{ms}']\{\phi_s'\} + [D_{mm}']\{\phi_m'\} = \{0\} \tag{5b}$$

Even for large frequency changes, the global mode shapes usually do not change drastically. Hence, the baseline structure typically gives a good approximation for $\{\phi_s'\}$,

$$\{\phi_s'\} = \{\psi\} + \{\Delta\psi\} \tag{6}$$

where

$$\{\psi\} = -[D_{ss}]^{-1}[D_{sm}]\{\phi_m'\} \tag{7}$$

Substitution of Eqs. (6) and (7) into Eqs. (5) gives the nonlinear perturbation equation

$$[D_{ms}]\{\psi\} + [D_{mm}]\{\phi_m'\} + [\Delta D_{ms}]\{\psi\} + [\Delta D_{mm}]\{\phi_m'\} - ([D_{ms}] + [\Delta D_{ms}])([D_{ss}] + [\Delta D_{ss}])^{-1} \times ([\Delta D_{ss}]\{\psi\} + [\Delta D_{sm}]\{\phi_m'\}) = \{0\} \tag{8}$$

The last term of Eq. (8) contains the inverse of an unknown matrix and hence makes the problem complicated. An iterative procedure is used to solve the nonlinear equation.

Numerical Example

As an example, a uniform curved shell segment[2] is considered. The axial length and outer radius are 76.2 mm. The arc angle is 45 deg and the plate thickness is 3.17 mm.

Received Aug. 24, 1984; revision received Nov. 16, 1984, presented as Paper 85-0730 at the AIAA/ASME/ASCE/AHS 26th Structures, Structural Dynamics and Materials Conference, Orlando, FL, April 15-17, 1985.

*Project Engineer. Member AIAA.

The design goal is to modify the fifth mode of chordwise bending. The translational vibration of the top midpoint will be decreased. Two top points on each side are used as reference points. The master set includes these 3 degrees of freedom and 357 unconstrained degrees of freedom are included in the slave set. The remaining modes are allowed to move without constraint.

The perturbed elements are divided into 8 design groups as shown in Fig. 1. Plate thicknesses of the groups are the design variables. The total weight of the structure is to be minimized.

Case 1: Mode Changed, Frequency Fixed

The vibration amplitude of the top midpoint, $-.046642$, will be decreased by 20% to -0.37314 with the frequency unchanged. The amplitude of the two side points will remain unity as reference points.

The predicted fractional thickness change $[\Delta h/h]$ is shown in Table 1. Because the system is symmetric, every two groups have the same values. The reanalysis results at each iteration are given in Table 2.

Table 1 Case 1: design variables ($\Delta h/h$)

	Group			
	1,8	2,7	3,6	4,5
Baseline	0.	0.	0.	0.
Linear	+0.300	−0.150	−0.150	+0.140
Nonlinear				
First	+0.277	−0.146	−0.104	+0.245
Second	+0.277	−0.141	−0.092	+0.244
Third	+0.277	−0.141	−0.091	+0.244

Table 2 Case 1: characteristic changes

	Mode shape top midpoint	Frequency, $\omega_5 \times 10^{-4}$
Baseline system	−0.46642	3.3451
Design goal	−0.37314 (−20%)	3.3451 (0%)
Linear	−0.34253 (−27%)	3.1565 (−6%)
Nonlinear		
First	−0.36329 (−22%)	3.3168 (−1%)
Second	−0.37270 (−20%)	3.3443 (−0%)
Third	−0.37314 (−20%)	3.3451 (0%)

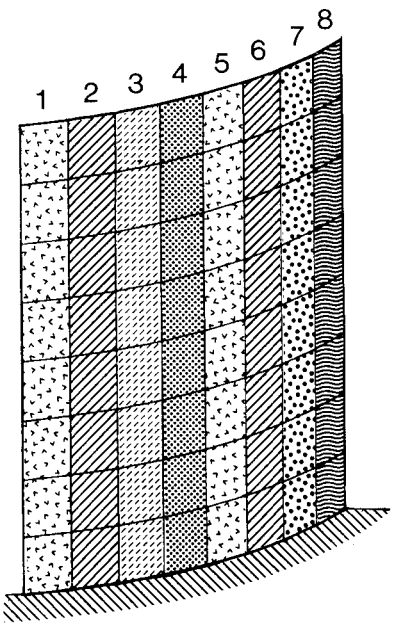

Fig. 1 Uniform shell and design groups ($E = 6.1 \times 10^4$mPa, $\nu = 0.31$, $\rho = 2.7 \times 10^{-9}$N·s^2/mm^4).

Table 3 Case 2: design variables ($\Delta h/h$)

	Group			
	1,8	2,7	3,6	4,5
Baseline	0.	0.	0.	0.
Linear	−0.300	−0.200	+0.174	−0.300
Nonlinear				
First	−0.326	−0.183	+0.214	−0.353
Second	−0.333	−0.167	+0.222	+0.358
Third	−0.333	−0.165	+0.223	+0.358

Table 4 Case 2: characteristic changes

	Mode shape top midpoint	Frequency, $\omega_5 \times 10^{-4}$
Baseline system	−0.46642	3.3451
Design goal	−0.37314 (−20%)	4.3486 (+30%)
Linear	−0.37173 (−20%)	4.0949 (+22%)
Nonlinear		
First	−0.36694 (−21%)	4.2858 (+28%)
Second	−0.37094 (−20%)	4.3446 (+30%)
Third	−0.37180 (−20%)	4.3486 (+30%)

Case 2: Mode Changed, Frequency Changed

The frequency will be increased by 30% along with the mode shape change, which means that the baseline frequency of 3.3451×10^4 will be changed to 4.3486×10^4. Table 3 shows the rates of thickness changes of design groups. The reanalysis results are given in Table 4.

Conclusions

A structural redesign method using dynamic condensation gives accurate results for changes of modal characteristics. The main advantage is that the final formulation is expressed in terms of structural design variables only and no design sensitivities for dynamic characteristics are required. Hence, the solution is simple even for large systems.

The method is efficient for redesign because it requires only a single finite element analysis of the baseline system, which gives the necessary information for the later redesign procedures. The solution converges rapidly for both mode shape and frequency changes.

The master set consists of the specified degrees of freedom and is chosen from those that have large energy.[3] The energy level in each degree of freedom is different from mode to mode. Hence, the master set is the union of sets for the modes when several modes are to be modified.

Acknowledgment

This research was funded by the MacNeal-Schwendler Corporation, Los Angeles, Calif., and this support is gratefully acknowledged. The author wishes to thank the Engineering Staff of MSC for their help during the work.

References

[1]Stetson, K.A. and Palma, G.E., "Inversion of First Order Perturbation Theory and Its Application to Structural Design," *AIAA Journal*, Vol. 14, April 1976, pp. 454-460.

[2]Stetson, K.A. and Harrison, I.R., "A Study of Structural Redesign by Finite-Element Inverse Perturbation of Vibration Modes," United Technologies Research Center, East Hartford, Conn., Rept. R80-191942-1, Jan. 1980.

[3]Kim, K.O., Anderson, W.J., and Sandstrom, R.E., "Nonlinear Inverse Perturbation Method in Dynamic Analysis," *AIAA Journal*, Vol. 21, Sept. 1983. pp. 1310-1316.

[4]Kim, K.O. and Anderson, W.J., "Generalized Dynamic Reduction in Finite Element Dynamic Optimization," *AIAA Journal*, Vol. 22, Nov. 1984, pp. 1616-1617.

[5]Leung, Y.T., "An Accurate Method of Dynamic Condensation in Structural Analysis," *International Journal of Numerical Methods in Engineering*, Vol. 12, 1978, pp. 1705-1715.

[6]Paz, M., "Dynamic Condensation," *AIAA Journal*, Vol. 22, May 1984, pp. 724-727.

Strength Prediction of a Mechanically Fastened Joint in Laminated Composites

Charles E.S. Ueng* and Kai-da Zhang†
Georgia Institute of Technology, Atlanta, Georgia

Introduction

RECENTLY, advanced composites have been widely used in many aerospace structures. Just as in any structure made of conventional materials, a load must be transmitted from one member to another through an efficiently and effectively designed joint. This is particularly important for composite structures because any weight saving through the use of modern composites can be easily eroded by improper or overdesigned joints. Mechanically fastened joints can provide certain advantages, such as ease of inspection, no need for special surface treatment, and tolerance to the effects of environmental loading. The authors[1,2] have recently obtained compact analytical solutions, including the frictional effect, for the stresses around a pin-loaded hole by stress functions of complex variables. The results indicate that, in general, the normal stress does not follow a cosinusoidal distribution for orthotropic material and the presence of friction may cause a significant effect to the stress distribution. In this Note, those solutions [1,2] are used for computing the stresses along a characteristic curve [3,4] and then the Yamada-Sun[5] criterion is applied to evaluate the ultimate load and the failure mode. The results are compared with the available experimental data.[6-8]

The advantages of this approach are: 1) the effect of the friction on the strength prediction is included; 2) the strength evaluation of a mechanical joint involving an arbitrarily orthotropic composite material can be carried out without complicated computation as long as the basic material properties are given; and 3) the method is easily adaptable for the case where the direction of the pin load does not coincide with the direction of one of the material principal axes.[2]

Analysis

The following assumptions are made for deriving a simple and reasonable prediction of the failure pin load: 1) only two-dimensional stress analysis is considered and the effect of delamination is ignored; 2) the laminate is bonded perfectly; 3) distribution of the pin load along the plate thickness is uniform; and 4) a final failure occurs when a combination of stresses in any lamina of this laminate reaches the critical value. The Yamada-Sun criterion is used to predict the ultimate strength, that is,

$$(\sigma_{xi}/X)^2+(\tau_i/S_c)^2=\ell^2\begin{cases}\ell^2<1, & \text{no failure}\\ \ell^2\geq 1, & \text{failure}\end{cases} \tag{1}$$

Received Sept. 7, 1984; revision received March 4, 1985.

*Professor, Engineering Science and Mechanics.

†Instructor, Northwestern Polytechnical University, Xian, Saanxi, China.

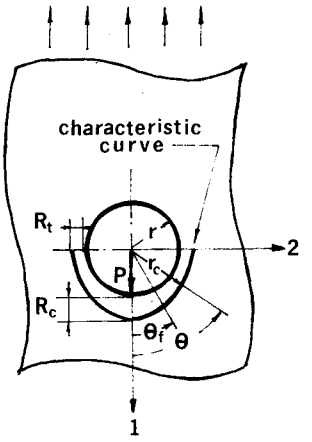

Fig. 1 A sketch of the characteristic curve (D = 2r).

where σ_{xi} and τ_i are the normal stress along the direction of fiber and the shear stress in the i^{th} lamina, respectively, X the ply longitudinal strength, and S_c the ply shear strength measured from a symmetric cross-ply laminate. It is noted that σ_{xi} and τ_i are the stresses at points located on a characteristic curve whose equation is represented by

$$r_c=r+R_t+(R_c-R_t)\cos\theta, \quad -\pi/2\leq\theta\leq\pi/2 \tag{2}$$

as shown in Fig. 1, where r is the radius of the loaded hole and R_t and R_c the characteristic lengths determined from experimental results. They depend only on the material itself.

For the strength prediction, we adopt the following approach in which the stress values around a loaded hole are multiplied by the ratio r/r_c in order to obtain the stresses around the characteristic curve. The reason is that the characteristic curve is located nearby the hole and the elasticity effect of this small region between the hole edge and the characteristic curve can therefore be ignored. In doing so, the tedious computational work can be avoided. Based upon this approximation, the stresses around the characteristic curve can be simply presented as

$$\sigma_{rc}=\sigma_r r/r_c, \quad \sigma_{\theta c}=\sigma_\theta r/r_c, \quad \tau_{r\theta c}=\tau_{r\theta} r/r_c \tag{3}$$

where σ_r, σ_θ, and $\tau_{r\theta}$ are the normal stresses and shear stress around the pin-loaded hole, respectively. The detailed computational procedure and equations are available in Ref. 9.

Comparison with Experimental Results

The following constants adopted from Refs. 3, 4, and 10 are used in the evaluation of the failure load: $R_c=2.032$ mm (0.08 in.), $R_t=0.457$ mm (0.018 in.); friction coefficient $f=0.2$, and $S_c=2.5S$ where S represents the lamina shear strength obtained by testing single plies. The predicted failure mode is determined as suggested by Chang et al.[3] as follows:

$-15<\theta_f<15$ deg, bearing failure mode

$30<\theta_f<60$ deg, shearout failure mode

$75<\theta_f<90$ deg, tension failure mode

where θ_f is the angle for a point where the combined stress reaches the critical value. Tables 1-3 list the experimental and analytical results for the failure loads or stresses of two kinds of laminates made of the same fiber but with different matrix materials. (Note: All of the tests quoted in Tables 1-3 were made at room temperature and under static load up to failure.)

For considering the effect caused by friction, the ultimate bearing strengths for some laminates are calculated under dif-